Author's response to anonymous referee #1

Major Points:

-Point-0, L37-43 A more detailed discussion of more complex and time consuming numerical models (based on the RANS equations, e.g. Abadie et al., 2010; Clous & Abadie, 2019) is needed. This would help the Readers in comparing the approach proposed by the Authors with the ones available in the scientific literature (see also Point-1).

Answer:

- RANS equations have been mentioned and the suggested references have been added. The paragraph has been rewritten(L33-55).
- Concerning the computation time, direct comparison is not feasible, it depends on the spatial and temporal resolution. We add a section about this topic (L400-403).

-Point-1, Abstract and L43-44 "However, the complexity of this phenomenon causes such models to be either computationally inefficient or unable to handle the overall process.", "The assessment of natural hazards requires predictive numerical models that are able to sufficiently reproduce the studied phenomenon while being efficient in terms of computational resources.". These sentences are quite subjective and are partially related to the previous point raised by the Reviewer. It is certainly true that a predictive numerical tool should be as "computationally efficient" (i.e. fast) as possible. Nevertheless, the first quality for a numerical model, to be considered a predictive tool to assess natural hazard, it should be related to the ability in reproducing adequately the complex phenomena at hand. Thus, the computational efficiency cannot be a strength of the model "per se". On the other hand, a good trade-off between a sufficient/good (but not perfect) reproduction of the phenomenon and a fast computational time is essential when real-time tsunamis early warning systems are considered (e.g. Titov et al., 2005; Cecioni et al., 2011).

Answer:

- The paragraph has been rewritten (L34-68). Nevertheless, in general, the comments of both reviewers show that they understand the statement of the balance "correctness-efficiency" and that we had to make a choice of the level of approximation. We chose the non-linear shallow water equations (without multiple add-ons), hence, the inherent approximations. We won't discuss in the paper the well-known limitations of this approach.

-Point-2, Section 3.1.3 The perfectly elastic collision approach, although clearly not correct from a physical point of view, seems to be a clever one for modelling the momentum transfer, at least as a first approach. Nevertheless, few aspects need to be clarified and/or better discussed. First: the Authors claim that the traditional approach for modelling the momentum transfer (e.g. Kelfoun et al., 2010; Xiao et al., 2015) entail undesired user-defined coefficients; on the other hand, also in the proposed approach at least one user-defined calibration coefficient (SF) is needed. Thus, a deeper discussion, as well as more details on the advantages that this approach can bring if compared with the traditional ones, are expected. Second: Figure 2 is not completely clear (and, as a secondary aspect, this Figure has a very poor quality and resolution, please improve it). A discussion of these 2 panels, which likely represent a key aspect of the current approach, is missing in the text. Finally, a more clear description of the Figure (in the legend the Authors refer to "eq. 34", the curves +50 -50 are present

in the legend but not described in the caption nor in the text, it is stated that the red line is not the best fitting curve but it is not clear how it has been obtained, etc.) is strongly recommended.

Answer:

- First: The description of the approach of Kelfoun et al. (2010) and Xiao et al. (2015) have been improved (L60-66).
- Second: The figure 2 has been updated (quality, legend) and the description has been improved (Fig.2; L223-230).

-Point-3, L235 Figures 3 and 4 are poorly described, please improve the description. A brief description of the tsunami generation, well represented by these Figures, can be of interest for the Readers.

Answer:

- The figure 3 has been improved and a more detailed description has been done (Fig. 3; L246-258)

-Point-4, L268-272 While describing Figure 5, the Authors point out that "the results from the numerical and physical models are on the same order of magnitude, which permits globally validating the different numerical models but does not allow discrimination between them". Which is certainly true. Nonetheless, one could wonder which parameter, among the landslide thickness (Figure 5a) and the depth-averaged slide velocity (Figure 5b), is more important for the proper momentum transfer modeling. A brief discussion on this would be appropriate.

Answer:

- While this suggestion is relevant, the investigation we performed to determine, in this particular case, which parameter has more influence on the wave amplitude was not applicable. Indeed, the thickness and the velocity of the landslide is directly linked to the parameters of the slide material and the apparatus. The realisation of this analysis would have required to simulate new scenarios, which is beyond the scope of this study.

-Point-5, L344 "We can underline that there is a better match with the runup height than with the wave amplitude" please provide a quantification of the discrepancies between numerical and experimental runup heights and wave amplitudes.

Answer:

- -we decided to remove the section concerning the runup, as it is a bit out of scope of the aim of the study and because of inconsistencies.

Minor Points:

L20-42: please add some missing references (e.g. Lynett & Liu, 2005; Panizzo et al., 2005; Abadie et al., 2010; Løvholt et al., 2015; Clous & Abadie, 2019):

- Some references added (L33-68)

L59: “wrong”, please choose another word or rephrase the whole sentence:

- Changed (L73)

L163: “ultrathin layer of water”, please provide more details also considering the option to add a figure with the numerical setup:

- We think a development of this concept isn’t relevant.

Figure 3: Numbers and symbols on the colormaps are too small, please improve it:

- Figure Improved (Fig. 3)

Figure 4: please provide more details of the considered numerical simulation in the caption:

- More detail in the text (L254-258). We won’t add more detail as the idea of this figure was to illustrate the cross-section of the 2.5D model.

L299: “more distantly”, please change.

- Changed (L316)

Author's response to anonymous referee #2

Specific comments:

A motivation for the Author to use the simplified model is to save computational resources (L44). Therefore, it would be good to discuss this aspect in the manuscript (e.g. what were the used computer resources, what was the computation time of typical run, what is the cell size, etc.).

Answer:

- We add a section about computational resources (L400-403).

L19: A landslide can also be partially submerged.

Answer:

- Corrected (L23-24)

L38: Smoothed Particle Hydrodynamics is a solver, not a set of governing equations. Modelling the generation of subaerial landslide-generated tsunamis with the shallow water equations was state-of-the-art 15-10 years ago. I feel the way this is written is slightly misleading. Further, more appropriate governing equations for the problem are the RANS equation with turbulence closure, amongst others (LES, DNS, Euler equations).

Answer:

- RANS equations have been mentioned. The paragraph has been rewritten (L33-55).

L41: It is unclear what the Authors mean by "full 3D", Smoothed Particle Hydrodynamics can also address the problem in 3D? Also, coupled approaches are a common trend nowadays, which are not covered, see e.g. Tan et al. (2018). A numerical landslidetsunami hazard assessment technique applied on hypothetical scenarios at Es Vedrà, offshore Ibiza. Journal of Marine Science and Engineering 6(4):1-22 and other two-layer models such as Ma et al. (2015). A two-layer granular landslide model for tsunami wave generation: Theory and computation. Ocean Modelling 93:40-55. See also the comprehensive review of Yavari-Ramshe and Ataie-Ashtiani (2016). Numerical modeling of subaerial and submarine landslide-generated tsunami wavesâˇA ˇTrecent advances and future challenges. Landslides for a more holistic overview of numerical options.

L41: What is a less classical hybrid approach? Please elaborate.

Answer:

- Coupled approaches have been mentioned and some references added (L33-55).
- The paragraph has been rewritten (L33-55).

L43: Why do the predictive methods do need to be numerical, why not physical model studies other methods?

Answer:

- They don't. Sentence rewritten (L45)

L45: Again, the application of the shallow-water equations for landslide-tsunami generation, at least for subaerial ones, was state-of-the-art around 15 years ago as they exclude, in the general form, key physical concepts such frequency dispersion. It should also be clearer from the text which shallow-water equations are discussed (nonhydrostatic, non-linear, linear)?

Answer:

- The comments of both reviewers show that they understand the statement of the balance "correctness-efficiency" and that we had to make a choice of the level of approximation. We chose the non-linear shallow water equations (without multiple add-ons), hence, the inherent approximations and incomplete physics (such as frequency dispersion). We won't discuss in the paper the well-known limitations of this approach.
- Some precision concerning the shallow water equations have been added (L70, L100).

L50: It is unclear what the Authors mean by "drag-like equations", please give more details.

Answer:

- The paragraph has been enhanced (L60-68).

L59: "method is obviously wrong from a physical perspective". This is supposed to be a research article, not an Engineering report, so the introduction of physical flawed concepts is slightly questionable. Please comment.

Answer:

- We have renamed our approach as "perfect" collision as the term "perfectly elastic" was misleading. It is "perfect" in the sense that there is no dissipation, neither the momentum nor the kinetic energy.
- Rewritten in the text (L71-72).

L86: Again, the Authors need to be more precise which shallow-water equations they apply. Some of them are appropriate, at least for tsunami propagation. None of them is appropriate for subaerial landslide-tsunami generation in my view.

Answer:

- Some precision concerning the shallow water equations have been added (L70, L100).
- The comments of both reviewers show that they understand the statement of the balance "correctness-efficiency" and that we had to make a choice of the level of approximation. We chose the non-linear shallow water equations (without multiple add-ons), hence, the inherent approximations and incomplete physics (such as frequency dispersion). We won't discuss in the paper the well-known limitations of this approach.

L120: The descriptions in the text does not fit with the term “relative density”, which indicates one density relative to the other, rather than one density minus another density. The sentence after (“Since each…”) does not resolve this confusion well.

Answer:

- The term has been changed to “apparent density” (L133 and Notation).

L163: I understand that the Authors introduce a small water layer to avoid zeros in the water depth array. In other words, the Authors introduce unphysical boundary conditions to avoid singularities/a numerical issue. This needs a better justification in my view. The fact that this water layer is transferred into a viscous layer does not really resolve this questionable approach. A better option to deal with a numerical issue is on the numerical side, not by compromising the physics.

Answer:

- This is justified because using this approach, there is no special need to introduce new equations for wet-dry transition.

L184: More unphysical behavior is introduced with the elastic collision principles, research should give new physical insight into phenomena, not to opposite. I invite the Authors to comment.

Answer:

- We have renamed our approach as “perfect” collision as the term “perfectly elastic” was misleading. It is “perfect” in the sense that there is no dissipation, neither the momentum nor the kinetic energy.

Eq. (31): A fitting parameter is introduced. How would the solution look like without fitting parameters? This is a weakness that the maximum slide needs to be known a priori to compute the slide behavior and landslide-tsunami afterwards. Can the Authors discuss where they would know this parameter from in a real scenario?

Answer:

- In fact, the maximum slide thickness is not a manual input. During the simulation, the landslide maximum thickness is tracked (and registered) in the numerical equivalent location of the Cam1 (Figure 1). In the case of a real scenario, the same principle will apply. The operator only need to point out where this value is numerically measured.
- This aspect has been precised in the text (L225).

L226: I am not sure if the Reader is interested in a comparison which is difficult to performed. It looks like this came out of a discussion within the Author team. And it would be better suited in the Discussion section. I suggest removing this paragraph.

Answer:

- Paragraph removed (L238-244)

The water surface elevation in the last screenshot in Fig. 4 looks rather unphysical.

Answer:

- This is due to the approximation inherent to the shallow water equations.

L250: The Authors aim to predict landslide-tsunamis in nature, by fitting their numerical result to the one in the laboratory. How do the Authors deal with the fact that laboratory granular slide deposits do not represent the behavior in nature at all due to scale effects (see e.g. Kesseler et al. (2020). Grain Reynolds number scale effects in dry granular slides. Journal of Geophysical Research-Earth Surface 125(1):1-19.)? Would their model still be able to predict the phenomenon in nature?

Answer:

- In this paper, we present the comparison between our model and a specific physical experiment. It shows that when we implement exactly the measured rheological parameters in our model (for granular flow), the behaviour of the landslide is correct. Moreover, speaking about the dry case, our model was by no mean modified to fit the physical experiment. The isotropic Coulomb rheology was used and the friction angles were implemented, that's it. Thus, we think that it is a robust approach to validate a numerical model.
- While we won't discuss the scale effects on the physical experiment conducted in Miller et al. (2017) here, the fact that they used slide masses greater than 500 kg (while Kesseler et al. (2020) investigated side masses between 1 and 110 kg), place this particular study on the "positive" side.
- Back analysis of real cases are also a way to validate numerical models, but "playing" with the input parameters and tuning the code was not the topic of this paper. We have already used our model in real case study, either prospective or in back analysis, and showed good capacities. Unfortunately, at this time, the code was not in its actual state (e. g. the momentum transfer was not implemented). (e. g. Franz, M., Rudaz, B., Jaboyedoff, M. & Podladchikov, Y. (2016). Fast assessment of landslide-generated tsunami and associated risks by coupling SLBL with shallow water model. Proceeding of the GEOVancouver 2016 conference; Franz, M., Jaboyedoff, J., Podladchikov, Y. & Locat, J. (2015). Testing a landslide-generated tsunami model. The case of the Nicolet Landslide (Québec, Canada). Proceeding of the GEOQuébec 2015 conference). The use of the present state model in real case scenarios will be presented in a future paper to address this crucial point, on which we agree.

L258: In the Voellmy rheology a back analysis is performed to fit the laboratory experiment. How would this be done if applied to real cases?

Answer:

- The Voellmy rheology is widely used to simulate snow and rock avalanches. The parameters used in prospective study are often based on regional back analysis cases (e. g. Hungr, O. & Evans, S.G. (1996). Rock avalanche runout prediction using dynamic model. Landslides.).

L271: “same order of magnitude” means up to a factor of 10 difference. Is this really what the Authors try to state? How useful is a numerical simulation modeling the phenomenon with a difference of up to a factor of 10? Further, in Fig. 5 the mass between the physical and numerical slides seems to be very different. Is the mass at all conserved in the numerical model?

Answer:

- “same order of magnitude” has been changed in the text (L288-290).
- Yes, the mass is conserved in the numerical model. The difference in fig. 5 are due to an incomplete graph (stops at 3.2 s) and the fact that thickness of the landslide in the physical experiment is expended (bouncing beads). This is not reproduced numerically.

L323: It is unfortunate that the Authors include 5 and 10 cm water depth in their analysis, which are cases in the region of significant scale effects (see the technical literature where h > 0.200 m is specified to avoid significant scale effects for granular slides). The model does not include all physics to represent scale effects (e.g. surface tension). This is a limitation of the study. E.g. how can the Authors be sure that scale effects are not responsible that their simulation fits well with the experimental results at 5 cm water depth?

Answer:

- We think that the scale effect is not dominant in this case. This is highlighted by the fact that fairly good correspondence between the laboratory and the numerical simulation are present over and under the 0.2 m threshold Referee #2 mentions.

Fig. 9: The Authors need to apply a parameter to proper judge the agreement between the laboratory and numerical results, e.g. a normalised Root Mean Square Error (nRMSE) relative to the amplitude, or similar.

Answer:

- The nRMSE is too dependent to the location in time of the wave or to the size of the windows in which it would be computed. We will not perform it.

Fig. 9: The weaknesses of the shallow-water equation approach become now obvious in the wave profiles, e.g. frequency dispersion is not modelled resulting in significant deviations between numerical and laboratory results. A detailed discussion about frequency dispersion is required, see e.g. Ruffini et al. (2019) Numerical modelling of landslide-tsunami propagation in a wide range of idealised water body geometries. Coastal Engineering 153:103518 or similar studies where landslide-tsunamis are modelled with and without frequency dispersion. The relevance of frequency dispersion on landslide-tsunami propagation is very well known and documented.

Answer:

- The comments of both reviewers show that they understand the statement of the balance “correctness-efficiency” and that we had to make a choice of the level of approximation. We chose the non-linear shallow water equations (without multiple add-ons), hence, the inherent

approximations and incomplete physics (such as frequency dispersion). We won't discuss in the paper the well-known limitations of this approach.

L343: The wave train is not simulated because the model is unable to model frequency dispersion. This should be mentioned/discussed.

Answer:

- Also due to the lack of breaking wave in the model. Mentioned in the text and paragraph rewritten (L409-415).

Figure 11 (now Fig. 10): The data of the numerical simulations are on the un-safe side, which maybe an issue for hazard assessment.

Answer:

- The data of the numerical simulations are indeed a little lower (smaller Am) than the lab data and it would have been beneficial for hazard assessment to be in the opposite case. Nevertheless, they stay within the +/-30% deviation from the Eq. (39) which is considered as a good fit (Heller et al., 2010).

L381: I cannot follow why the Authors state that their data are within 30%, it looks rather like a 50% deviation from Eq. (39)?

Answer:

- The dashed lines are strictly the Eq. (39) +/- 30%. It is obvious, for instance, if we check the plain line at $Am = 3$. The upper dashed line is at $Am = 4$ (3+(3*0.3)) and the lower dashed line is at $Am = 2$ (3-(3*0.3). Therefore, as the data are within the dashed lines (except for 0.05m) they are within +/- 30%. The maximum relative wave amplitude Am is a function of the impulse product parameter P. We also should keep in mind that the figure 11 uses the same axis lengths as in Miller et al. (2017). The figure presented in Heller et Hager (2010) has the P axis that stops at 9, which means that the relationship from Eq. (39) is not valid after this point. Nevertheless, the numerical data for a water depth of 0.05 m is not so distant from the laboratory data.

L384: The fact that the model cannot consider breaking also implies that it cannot consider the impact crater, etc. It would be good to mention/discuss these aspects as well.

Answer:

- While it is true that the model cannot handle breaking, it is not true that it cannot handle the impact crater, as long as the steepness of the water surface is not steeper than "sub-vertical".
- Paragraph updated (L405-409).

L388-293: The argumentation in this section is misleading. The main reason for the absence of the wave train is not breaking, it is the inability of the shallow-water equation (in the form used by the Authors) to model frequency dispersion.

Answer:

- Also due to the lack of breaking wave in the model. Mentioned in the text and paragraph rewritten (L409-415).

L403: The Conclusions should be understandable on their own. I suggest starting with a brief motivation and method of the study before summarising the conclusions.

Answer:

- A new paragraph has been added at the begging of the section (L428-432).

L410: I do not agree that this statement is appropriate. The wave in the numerical model behave not similar to the ones in the experiments due to the absence of frequency dispersion in the numerical model. I also do not agree with the conclusion "the choice to transfer the momentum through the simple perfectly elastic collision principle is verified to be relevant." I cannot recall where this has been shown in the article? Please clarify and/or update the Conclusions.

Answer:

- The comments of both reviewers show that they understand the statement of the balance "correctness-efficiency" and that we had to make a choice of the level of approximation. We chose the non-linear shallow water equations (without multiple add-ons), hence, the inherent approximations and incomplete physics (such as frequency dispersion). We won't discuss in the paper the well-known limitations of this approach.
- We consider the results sufficiently good from this point of view.

L416: The 211 experiments have been performed by Heller and Hager (2010), 137 ones by Fritz et al. (2002) as well as 86 ones by Zweifel (2004) (see Heller and Hager, 2010).

Answer:

- This has been corrected (L445-446)

L417: "… our model is further strengthened by the fact that the results of our model also fit well with those experiments." I disagree, this statement contradicts Fig. 11. The trend of the numerical data is very different to the trend given by Eq. (39), so there is a systematic difference, and the discrepancy is up to 45%.

Answer:

- The dashed lines in Figure 10 are strictly the Eq. (39) +/- 30%. It is obvious, for instance, if we check the plain line at *Am* = 3. The upper dashed line is at *Am* = 4 (3+(3*0.3)) and the lower dashed line is at *Am* = 2 (3-(3*0.3). Therefore, as the data are within the dashed lines (except for 0.05m) they are within +/- 30%. The maximum relative wave amplitude *Am* is a function of the impulse product parameter P. We also should keep in mind that the figure 11 uses the same axis lengths as in Miller et al. (2017). The figure presented in Heller et Hager (2010) has the P axis that stops at 9, which means that the relationship from Eq. (39) is not valid after this point. Nevertheless, the numerical data for a water depth of 0.05 m is not so distant from the laboratory data.

Suggested grammatical corrections and minor points:

Title: The title includes some repetitions and should be written more concise:

- We keep it as it is.

L8: A landslide-generated tsunami is a water wave, it does not involve “landslide dynamics”, please rephrase;

L9: Grammar issue, the plural form does not match the singular form used in the previous sentence.

- The sentence has been rewritten (L8-10)

L12: Please write “the shallow water…”:

- Done (L13)

L16: Please write “performs best…”:

- Done (L17)

L19/20: Same issue as on L8:

- Done (L22)

L28: Landslide-generated tsunamis are not observed on plains, they are observed in the water body. Please rephrase:

- Rephrased (L30)

L42: Please write “an advanced…”:

- Done (L54)

L49: Please follow Harvard style by adding brackets ahead and after the year.

- Done (L60)

L54: “automatically” is not a good choice, it indicates that the applier needs to do nothing in the simulation.

- Deleted (L67)

L57: Consider replacing “specification” with “framework”:

- Done (L71)

L62: Please write “to wave generation”.

- Done (L76-77)

L65: “Moreover, the granular flow is gravitationally accelerated, which is a relevant aspect to test the behaviour of the numerical model.” It is not fully clear what the Authors try to state with this statement, many laboratory slides are accelerated by gravity.

- Yes, that’s true. We chose one of them, which in this study, is the one developed by Miller et al. (2017).

L68: “the comprehensive phenomenon of” is not necessary:

- Deleted (L83)

L71: Please replace “but” with “and”:

- Done (L86)

L73: The aluminium plate and the slope are not part of the flume, they are built into the flume, please rephrase:

- Rewritten (L88)

L75: It is common practice to write parameters in italic style in research articles, so please write h in italic and also all other parameters in the text, tables and figures (e.g. X in Figure 1). On the other hand, numbers (e.g. L152) must not be written in italic:

- It has been changed in the whole document.

L79: Please replace “to be” with “as”:

- Don (L94)

L85: Either write “an experiment” or “the experiments”:

- Done (L99)

L91: Please check the numbering style for equations and apply this style consistently throughout the manuscript:

- It has been corrected in the whole document.7

L97: Please check how “Section” is abbreviated (I do not think “sect.” is the correct abbreviations) and apply it consistently through the manuscript:

- Done (L111, L309)

L102: Please follow Harvard Style:

- Done (L116)

L117: “sin”, “cos” and “tan” should not be written in italic, here and throughout the manuscript:

- Done

L142: Please add “the” in front of velocity:

- Done (L153)

L144: The page reference can be dropped, the relation between Chezy and Manning Coefficient is undergraduate student material:

- Page reference dropped (L155)

Eq. (16): The writing style of d1/3 seems incorrect, also the number on L154 should be written as subscript.

- Style changed (L160)

L151: Please write “stress at which the slide starts or stops to move”:

- Changed (L162-163)

L180/1: Please move “from our point of view” without the brackets after “coefficients”:

- Corrected (L190-191)

L206: Please write “Eqs. (29) and (30)”, also on L230 and L314:

- Done (L217, 331)

Figure 2 (and the figures in general): Can the quality of the figures be improved in a professional software such as Adobe Illustrator, etc.? It looks like some of the figures are simple exported from Excel. Also please follow the consistent writing style (e.g. parameters in italic):

- The figures have been improved and the writing style has been harmonised (all figures)

L220/1: There are Grammar issues here, the Authors give the impression that Am = 0 in Miller et al. (2017) and it is also unclear what the Authors try to state with “not the best fitting curve”. Why?

- The legend has been improved as well as the text and the caption. (Fig. 2; L227-235)
- It is not the best fitting curve regarding only phenomenon, but it is the best for landslide and water.

The Text in Fig. 3 is unreadable small:

- Figure enhanced (Fig. 3)

Table 1: Please do not use abbreviations, but rather increase the width of the table:

- Full words written (Tab. 1)

L264: The presentation of the paragraph can also visually be improved, e.g. by intending the first line of the paragraph. Here and throughout the article:

- We have followed the guidelines

L276: Please write “versus” rather than “vs.”:

- Done (L294)

L281: Please drop “the” in front of best:

- Dropped (L296)

P13 at the bottom: Please avoid such free spaces (e.g. by moving the figures), also on P16:

- This will be performed for the very last version of the manuscript

L292: Please drop the in front of sect. and use the correct abbreviation for Section:

- Done (L309)

Figures 7/8: The text should not be written in italic. Please also write the full term for “w/o”:

- Done (Fig.7, Fig.8)

L315: Please replace “through” with “to”:

- Done (L332)

L316: Please drop one of the 8:

- Done (L333)

L317: Please write “a result”:

- Wrote “the” (L333)

L322: Please write “This section investigates the momentum transfer between the slide and the generated wave.”:

- Done (L339)

Fig. 9: Again, there are some issues here how the parameters/numbers are written.

- Corrected (Fig.9)

Fig. 10: The same issues as elsewhere. Also replace “@” with “at” :

- Figure deleted

L349: I do not think the explanation “The coloured: : :” is needed given that this is visible in the Notation. Similar statements can be dropped in figure captions elsewhere:

- This particular caption has been removed.
- The unneeded explanations have been removed from the other figures’ captions (All Figs.)

L357: Please write “Am is defined…”:

- Done (L374)

L364: Please drop “reservoir and” as there was not variation in the reservoir:

- Done (L381)

Figure 11 (Now Fig. 10): Is it possible to better highlight the legend in the figure e.g. by adding a frame? The symbols in the figure may be mixed up with the real data:

- A frame has been added (Fig. 10)

L414: Please write “the impulse product parameter particularly…”, there is only one:

- Corrected (L444)

L424: Please write “from all co-authors”:

- Done (L455)

Notations:

- Done

References: Please remove inconsistencies such as inconsistent use of upper and lower case letters in the article titles (e.g. :L440, L534, etc.), abbreviation and no abbreviation of Journal titles, typos (e.g. L518 “genrated”), etc.:

- Done

An efficient two-layer landslide-tsunami numerical model: effects of momentum transfer validated with physical experiments of waves generated by granular landslides

Martin Franz[1], Michel Jaboyedoff[1], Ryan P. Mulligan[2], Yury Podladchikov[1], W. Andy Take[2]

[1]Institute of Earth Sciences, University of Lausanne, Lausanne, CH-1015, Switzerland
[2]Department of Civil Engineering, Queen's University, Kingston, ON K7L 3N6, Ontario, Canada

Correspondence to: Martin Franz (mart.franz@gmail.com)

Abstract. ~~A landslide-generated tsunami~~The generation of a tsunami by a landslide is a complex phenomenon that involves landslide dynamics, wave dynamics and their interaction. Numerous lives and infrastructures around the world are threatened by thi~~s phnomenonese events~~.

Predictive numerical models are a suitable tool to assess this natural hazard. However, the complexity of this phenomenon causes such models to be either computationally inefficient or unable to handle the overall process. Our model, which is based on the shallow water equations, is developed to address these two problems. In our model, the two materials are treated as two different layers, and their interaction is resolved by momentum transfer inspired by elastic collision principles.

The goal of this study is to demonstrate the validity of our model through benchmark tests based on physical experiments performed by Miller et al. (2017). A dry case is reproduced to validate the behaviour of the landslide propagation model using different rheological laws and to determine which law performs ~~the~~ best. In addition, a wet case is reproduced to investigate the influence of different still water levels on both the landslide deposit and the generated waves.

The numerical results are in good agreement with the physical experiments, thereby confirming the validity of our model, particularly concerning the novel momentum transfer approach.

1 Introduction

The generation of a tsunami by a landslide ~~A landslide-generated tsunami~~ is a complex phenomenon that involves landslide dynamics, interactions between the landslide mass and a water body, propagation of a wave and its spread on the shore. A landslide could be either submarine, partially submerged or subaerial. Regions that combine steep slopes and water bodies are the most susceptible to landslide-generated tsunamis. For instance, fjords (*Åknes*: Ganerød et al., 2008; Harbitz et al., 2014; Lacasse et al., 2008, *Lituya Bay*: Fritz et al., 2009, Slingerland and Voight, 1979, Weiss et al., 2009), volcanos in marine environments (*Stromboli*: Tinti et al., 2008, *Réunion Island*: Kelfoun et al., 2010), and regions such as lakes and reservoirs in mountainous areas are prone to this phenomenon (*Chehalis Lake*: Roberts et al., 2013, *Vajont*: Bosa and Petti, 2011; Slingerland and Voight, 1979; Ward and Day, 2011; Kafle et al., 2019; *Lake Geneva*: Kremer et al., 2012, 2014, *Lake Lucerne*:

Schnellmann et al., 2006). On ~~plains~~lowland water bodies, landslide-generated tsunamis are also encountered when particular conditions exist, such as quick clays or glacio-fluvial deposit slopes (*Rissa*: L'Heureux et al., 2012, *Nicolet Landslide*: Jaboyedoff et al., 2009; Franz et al., 2015, *Verbois reservoir*: Franz et al., 2016).

Landslide-generated tsunamis severely threaten lives and infrastructures, as evidenced in Papua New Guinea in 1998, where a submarine landslide killed 2200 people (Tappin et al., 2008). To assess this hazard, predictive models must be used. These models can be separated into 3 different types: 1) empirical equations from physical models (Enet and Grilli, 2007; Heller et al., 2009., Fritz et al., 2004, Miller et al., 2017, Kamphuis and Bowering, 1970; Slingerland and Voight, 1979), 2) physical models reproducing site-specific setups (*Åknes*: Harbitz et al., 2014, *Vajont*: Ghetti, 1962 in: Ghirotti et al. 2013), and 3) numerical models. Numerical models can be governed by different sets of equations, such as ~~smoothed particle hydrodynamics (Heller et al., 2016; Wei et al., 2015),~~ shallow water equations (Simpson and Castelltort, 2006; Harbitz et al., 2014; Franz et al. 2013, 2015, 2016; Kelfoun 2011; Kelfoun et al., 2010; Mandli, 2013; Tinti~~t~~ and Tonini, 2013; Tinti et al. 2008), ~~and~~ Boussinesq equations (Harbitz et al., 2014; Løvholt et al., 2013; 2015), and RANS equations (Abadie et al., 2010; Clous & Abadie, 2019). ~~Furthermore, numerical models can be simulated in full 3D (Crosta et al., 2013), with a less classical hybrid approach (Xiao et al., 2015; Ward and Day, 2011), and with advanced multi-phase approach (Pudasaini, 2014; Kafle et al., 2019).~~

The assessment of natural hazards requires the use of predictive models, and in the case of numerical models, they need to be ~~that are~~ able to ~~sufficiently~~ reproduce sufficiently well the studied phenomenon while being efficient in terms of computational resources and easy to use and to implement. These requirements are indeed necessary for a tool designed for applied studies. From this point of view, the models based on RANS equations fulfil the first requirements but are particularly slow to run (Abadie et al., 2010; Clous & Abadie, 2019). On the other hand, models based on approximations such as shallow water equations and Boussinesq equations, and their free-surface nature, inherently imply a loss in the quality of the reproduction but permits to be used on standard computer with fast computational time. The difficulty to simulate the propagation of two different materials, the interaction between the landslide and the water, and the propagation on the shores using free surface models is often solved by coupled approaches (Tan et al., 2018; Ma et al., 2015; Harbitz et al., 2014; Løvholt et al., 2015) or with an advanced multi-phase approach (Pudasaini, 2014; Kafle et al., 2019). These hybrid approaches are a good trade-off between reproduction quality and efficiency but not regarding the ease of use. ~~The ease of implementation (few selected parameters) is also a great advantage. Models based on shallow water equations are a good compromise from this point of view (Franz et al. 2013). However, few of these models assess the whole phenomenon, i.e., simulating both the landslide propagation and the tsunami. To perform such an assessment, the model must handle complex behaviour, in particular sliding mass/water momentum transfer, wet-dry transition, and flooding.~~

Kelfoun et al. (2010) presented the *Volcflow* model, which has the ability to handle such behaviour and to address the quality-efficiency-usability requirement. In this model, the momentum transfer is performed by a set of ~~drag-like~~ equations that take into account the form drag and the skin friction drag, modified from the methodology reported by Tinti et al. (2006). Their approach is an elegant way to solve this type of problem; however, this method also relies on complex assumptions linked

with the incompatibility between the free-surface nature of the model and the hydrodynamic shape of the sliding mass and its associated drag coefficient. Xiao et al. (2015) simulated momentum transfer through a so-called "drag-along" mechanism, which. This approach is relevant, but requires the implementation of coefficients that are subject to interpretation. The two-phase mass flow model proposed by Pudasaini (2012) automatically simulates landslides and tsunamis within a single framework (Pudasaini, 2014; Kafle et al., 2019).

The numerical model we propose in this study is a two-layer model that combines a landslide propagation model and a tsunami model. The proposed numerical model is based on the non-linear shallow water equations in an Eulerian specification framework of the flow field. The transfer of momentum between the two layers is performed by assuming a perfectly elastic"perfect" collision, in the sense that that there is no dissipation, neither in momentum nor in kinetic energy. Although this method is obviously wrong from a physical perspective, it can be an optionThus, it appears to be appropriate to compute the momentum transfer between two materials in of which each cell has a certain velocity and a constant mass (or constant shape and constant density). This approach has the advantage of containing a limited number of coefficients to be implemented by the operator. The "lift-up" mechanism (i.e., the change in height of the water level due to bed rise) also contributes to the wave generation.

The aim of this study is to test the whole model (i.e., landslide and tsunami) and more specifically to examine the transfer of momentum between the two materials. Miller et al. (2017) provided a relevant benchmark test that highlights the momentum transfer through its effect on the granular flow deposit and on the amplitude of the generated wave. Moreover, the granular flow is gravitationally accelerated, which is a relevant aspect to test the behaviour of the numerical model.

2 Physical experiment of a granular landslide and wave

Miller et al. (2017) investigated the comprehensive phenomenon of landslide-generated tsunamis. In their study, the landslide, which consisted of a gravitationally accelerated granular flow, was simulated alongside the wave. The interaction between the two elements was of particular interest, and their reciprocal effects were highlighted. The momentum transfer obviously affected the wave behaviour andbut also influenced the landslide deposit.

Miller et al. (2017) and Mulligan et al. (2016) described the flume at Queen's University in Kingston (ON), Canada, where their physical experiments were conducted. This apparatusflume consisted of a 6.7 m aluminium plate inclined at an angle of 30°, followed by a 33-m-long horizontal section, and ending in a 2.4-m-long smooth impermeable slope of 27°; the width of the flume was 2.09 m. Nine different scenarios were tested, in which the water depth was varied from h = 0.05 to 0.5 m; one of these scenarios was tested without water. For each scenario, 0.34 m^3 (510 kg) of granular material was released from a box at the top of the slope. The granular material consisted of 3-mm-diameter ceramic beads, which had a material density of 2400 kg/m^3, a bulk density of 1500 kg/m^3, a static critical state friction angle of 33.7°, and a bed friction angle of 22°. The flat floor of the flume was composed of concrete. The bed friction angle was estimated to beas approximately 35°. The wave amplitudes were determined by 5 probes, and the slide characteristics were captured with a high-speed camera (Cam 1).

Formatted: Font: Italic

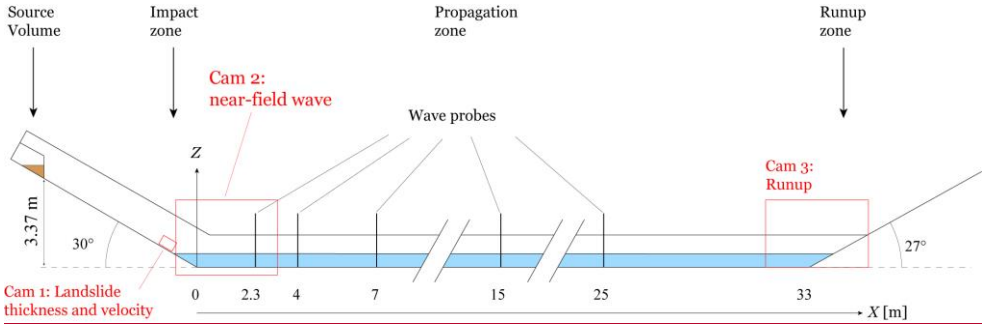

Figure 1: Sketch of the flume used in the physical model and implemented in the numerical model (modified from Miller et al., 2017).

3 Numerical model

The numerical model presented in this paper attempts to reproduce the experiments presented in Miller et al. (2017). The models for both the tsunami and the landslide simulations are based on the non-linear shallow water equations. The two layers are computed simultaneously (i.e., in the same iteration). The landslide layer is computed first and is considered as a bed change from the water layer (at each time step). The transfer of momentum also occurs at every time step.

3.1 Depth-averaged models

The model is based on two-dimensional shallow water equations:

$$U_t + F(U)_x + G(U)_y = S(U)\,, \qquad \textit{eq. 1}$$

where U is the solution vector and F and G are the flux vectors. These vectors are defined as follows:

$$U = \begin{bmatrix} H \\ Hu \\ Hv \end{bmatrix}, \qquad \textit{eq. 2}$$

$$F = \begin{bmatrix} Hu \\ Hu^2 + \frac{1}{2}gH^2 \\ Huv \end{bmatrix}, G = \begin{bmatrix} Hv \\ Huv \\ Hv^2 + \frac{1}{2}gH^2 \end{bmatrix}, \qquad \textit{eq. 3}$$

where H is the depth; u and v are the components of the depth-averaged velocity vector along the x and y directions, respectively; and g is the gravitational acceleration. The source term S differs for the landslide (Eq. 8) and tsunami models

(Eq. 19). Thus, the two formulations of the source term are specifically described in their respective sections (Ssect. 3.1.1 and 3.1.2). The conservative discrete form is expressed as follows:

$$U_{i,j}^{n+1} = U_{i,j}^{n} - \frac{\Delta t}{\Delta x}\left[F_{i+\frac{1}{2},j} - F_{i-\frac{1}{2},j}\right] - \frac{\Delta t}{\Delta y}\left[G_{i,j+\frac{1}{2}} - G_{i,j-\frac{1}{2}}\right] + \Delta t S_{i,j}^{n}, \qquad eq.\ 4$$

where $F_{i+\frac{1}{2},j}$ is the intercell numerical flux corresponding to the intercell boundary at $x = x_{i+\frac{1}{2}}$ between cells i and $i+1$ and $G_{i,j+\frac{1}{2}}$ is the intercell numerical flux corresponding to the intercell boundary at $y = y_{j+\frac{1}{2}}$ between cells j and j+1. The Lax-Friedrichs (LF) scheme defines these terms as follows (Franz et al., (2013); Toro, (2001)):

$$F_{i+\frac{1}{2},j}^{LF} = \frac{1}{2}\left(F_{i,j}^{n} + F_{i+1,j}^{n}\right) + \frac{1}{2}\frac{\Delta x}{\Delta t}\left(U_{i,j}^{n} - U_{i+1,j}^{n}\right), \qquad eq.\ 5$$

$$G_{i,j+\frac{1}{2}}^{LF} = \frac{1}{2}\left(G_{i,j}^{n} + G_{i,j+1}^{n}\right) + \frac{1}{2}\frac{\Delta y}{\Delta t}\left(U_{i,j}^{n} - U_{i,j+1}^{n}\right), \qquad eq.\ 6$$

This numerical scheme is chosen because of its non-oscillatory behaviour, its capacity to withstand rough beds, and its simplicity. See Franz et al. (2013) for more information concerning the choice of this numerical scheme.

3.1.1 Landslide model

The simulation of granular flow utilizes widely used rheological laws, among which the most commonly encountered are the Coulomb, Voellmy, and Bingham rheological laws (Iverson et al., 1997; Hungr and Evans, 1996; Longchamp et al. 2015; Pudasaini and Hutter, 2007; Pudasaini, 2012; Kelfoun, 2011, McDougall, 2006; Pouliquen and Forterre, 2001). The continuum equations used are the previously described equations. The source term *S* specifically governs the forces driving the landslide propagation:

$$S = \Delta t \begin{bmatrix} 0 \\ GR_x/\rho_s + P_x/\rho_s - T_x/\rho_s - M_{Tsx}/\rho_s \\ GR_y/\rho_s + P_y/\rho_s - T_y/\rho_s - M_{Tsy}/\rho_s \end{bmatrix}. \qquad eq.\ 7$$

where ρ_s is the landslide bulk density, T is the total retarding stress, and M_{Ts} is the momentum transfer from the water to the sliding mass. The driving components of gravity GR and pressure term P are defined as follows (Pudasaini and Hutter, 2007):

$$GR_x = \rho g H_s \sin\alpha_x \qquad GR_y = \rho g H_s \sin\alpha_y \qquad eq.\ 8$$

$$P_x = \rho g K_x \frac{\partial}{\partial x}\left(H_s{}^2 \cos\alpha_x\right) \quad P_y = \rho g K_y \frac{\partial}{\partial y}\left(H_s{}^2 \cos\alpha_y\right) \qquad eq.\ 9$$

where H_s is the landslide thickness, α is the bed slope angle, and K is the earth pressure coefficient. The density ρ is the ~~relative~~ apparent density of the landslide. This means that ρ is equal to the density of the slide ρ_s when the slide is subaerial and $\rho = \rho_s - \rho_w$ (density of the water) when the slide is underwater (Kelfoun et al., 2010; Skvortsov, 2005). Since each term is divided by ρ_s in Eq. (7), the relative nature of the density becomes effective. The total retarding stress T (T_x, T_y) is composed of the resisting force (frictional resistance) between the landslide and the ground. T differs depending on the chosen rheological law. The simple Coulomb frictional law *Coul* (MacDougall, 2006; Kelfoun et al., 2010; Kelfoun, 2011; Pudasaini and Hutter, 2007; Longchamp, 2015) is defined as follows:

$$T_x = Coul_x = \rho H_s (g \cos \alpha_x) \tan \varphi_{bed} \frac{u_s}{\|V\|} \qquad \textit{eq. 10}$$

$$T_y = Coul_y = \rho H_s (g \cos \alpha_y) \tan \varphi_{bed} \frac{v_s}{\|V\|} \qquad \textit{eq. 11}$$

where φ_{bed} is the bed friction angle and V (u_s, v_s) the slide velocity.

The Coulomb rheology can be used considering flow with either isotropic or anisotropic internal stresses. This difference is handled with the use of the earth pressure coefficient K (Hungr and McDougall, 2009; Kelfoun, 2011, Iverson and Denlinger, 2001; Pudasaini and Hutter, 2007). For the isotropic case, K is set to 1 (Kelfoun, 2011). In the anisotropic case, K designates whether the flow is in compression (positive sign) or in dilatation (negative sign), for which the coefficients are denoted as $K_{passive}$ or K_{active} (Hungr and McDougall, 2009; Pudasaini and Hutter, 2007), respectively. These terms are defined as follows:

$$K_{act/pass} = 2\frac{1 \pm \left[1 - (\cos \varphi_{int})^2 \left(1 + (\tan \varphi_{bed})^2\right)\right]^{\frac{1}{2}}}{(\cos \varphi_{int})^2} - 1 \qquad \textit{eq. 12}$$

$$K_x = \begin{cases} K_{active}, & \frac{\partial u_s}{\partial x} > 0 \\ K_{passive}, & \frac{\partial u_s}{\partial x} < 0 \end{cases} \quad K_y = \begin{cases} K_{active}, & \frac{\partial v_s}{\partial y} > 0 \\ K_{passive}, & \frac{\partial v_s}{\partial y} < 0 \end{cases} \qquad \textit{eq. 13}$$

where the variable φ_{int} is the internal friction angle.

The Voellmy rheology *Voel* combines Coulomb frictional rheology with a turbulent behaviour:

$$T_x = Voel_x = Coul_x + \rho \frac{u_s \|V\|}{\xi} \qquad \textit{eq. 14}$$

The first term is the Mohr-Coulomb frictional law, whereas the second term, which was originally presented by Voellmy (1955) for snow avalanches, acts as drag and increases the resistance with the square of the velocity. The turbulence coefficient ξ corresponds to the square of the Chézy coefficient, which is related to the Manning coefficient n by $C = H_s^{1/6}/n$ (MacDougall, 2006~~, p.76~~). The turbulence coefficient presented in Kelfoun (2011) is equivalent to the inverse of the turbulence

coefficient presented herein times g ($1/(\xi g)$). However, the physical basis of the Voellmy rheology is questionable (Fisher et al., 2012).

The Bingham rheology combines plastic and viscous rheological laws and is defined as follows (Skvortsov, 2005):

$$Plast_x = \frac{u_s}{\|V\|} T_0(1 + d_1) \qquad \textit{eq. 15}$$

$$Visc_x = \frac{2\mu_s u_s}{H_s\left(1-\left(\frac{d_1}{3}\right)\right)} \qquad \textit{eq. 16}$$

$$T_x = Bingham_x = Plast_x + Visc_x \qquad \textit{eq. 17}$$

where T_0 is the yield stress, which is the stress to overcome for at which the slide to starts or under which the slide stops to move; μ is the dynamic viscosity; and d_1 is the relative thickness of the shear layer. The latter variable is used to mimic the behaviour of Bingham flow that contains two distinct layers: a solid layer (the plug zone) and a shear layer (the shear zone, d_1). The determination of *d1* can be performed automatically (e.g., Skvortsov, 2005), but in this study, the use of a constant value provided better results.

3.1.2 Tsunami model

For the tsunami model, the source term *S* includes a consistency term and a momentum transfer term and is defined as follows:

$$S = \Delta t \begin{bmatrix} 0 \\ -H_w g 0.5 \frac{\partial}{\partial x}(B) + \frac{M_{Twx}}{\rho_w} \\ -H_w g 0.5 \frac{\partial}{\partial y}(B) + \frac{M_{Twy}}{\rho_w} \end{bmatrix}. \qquad \textit{eq. 18}$$

where H_w is the water thickness, *B is* the bed elevation (including the thickness of the sliding mass), and M_{Tw} is the momentum transfer from the slide to the water. The first term confers consistency to the model, which has been validated in Franz et al. (2013). The second term is the momentum transfer between the landslide and the water.

The wet-dry transition is realized by an ultrathin layer of water h_{min} that covers the whole topography (or the dry state). This permits the avoidance of zeros in the water depth array. Nevertheless, such a situation would lead to water flowing down the slopes after some iteration. Thus, to prevent this numerical artefact, the thin layer is governed by viscous equations (Turcotte and Schubert, 2002):

$$Q_x = \begin{bmatrix} F_i^{LF} \\ \rho_w \frac{q_x^2}{H_w} + \rho g \frac{1}{2} H_w \\ \frac{\rho_w u_w v_w}{H_w} \end{bmatrix} \qquad \textit{eq. 19}$$

where

$$q_x = -\left(sin\,\alpha_x + \frac{\partial}{\partial x}\,(H_w)\right)\frac{\rho_w g {H_w}^3}{3\mu_w} \qquad eq.\ 20$$

A threshold Re_{tr} is set for a Reynolds number that determines which set of equations (between viscous equations and shallow water equations) is used at each location in the tsunami model:

$$Re = \frac{\rho_w u_w H_w}{\mu_w} \qquad eq.\ 21$$

$$F^{LF}_{i+\frac{1}{2}} = \begin{cases} F^{LF}_{i+\frac{1}{2}}, & Re > Re_{tr}, \quad H_w > h_{min} \\ Q_x, & Re < Re_{tr}, \quad H_w < h_{min} \end{cases} \qquad eq.\ 22$$

3.1.3 Momentum transfer

The interaction between the landslide and the water proposed by Kelfoun et al. (2010) is based on a formulation of drag both normal and parallel to the displacement. This formulation involves two coefficients that need to be set manually, which is a manipulation this study aims to avoid. Moreover, they claim that their equation is a rewritten form of the equation presented in Tinti et al. (2006). However, in the latter, the depth of the landslide *Hs* is taken into account, whereas in Kelfoun et al. (2010), they account for the gradient of the landside depth.

In Xiao et al. (2015), the so-called "drag-along" approach also entails undesired ~~(from our point of view)~~ user-defined coefficients from our point of view and, when tried in our code, never fit the experiment data.

Regarding those two unsatisfying approaches, we decided to try an unconventional method. Based on a semi-empirical approach that fits the experimental data, the implementation of momentum transfer in our code is inspired by the ~~simple perfectly elastic~~rigid collision principle. This principle ~~does not generally apply in fluid dynamics, but it~~ is relevant because 1) the kinetic energy of the system is conserved, 2) a true interaction between particles is not ~~longer~~ possible in a model based on shallow water equations (free surface – no third dimension), and 3) the exchange of momentum between the landslide mass and the water is perfectly symmetric.

As a reference case, we consider velocity changes during the elastic collision of two rigid bodies. The conservation of momentum in elastic collision is given by the following expression:

$$m_s u_{sb} + m_w u_{wb} = m_s u_{sa} + m_w u_{wa} \qquad eq.\ 23$$

As the kinetic energy is also conserved, the following constraint applies:

$$\frac{1}{2} m_s u_{sb}^2 + \frac{1}{2} m_w u_{wb}^2 = \frac{1}{2} m_s u_{sa}^2 + \frac{1}{2} m_w u_{wa}^2 \qquad eq.\ 24$$

where u_w and u_s are the velocities for the 'water' and the 'slide' masses, respectively (subscript b = before collision and subscript a = after).

We assumed that the mass before collision remained constant after collision. Under this simplifying assumption, the two conservation equations can be used to solve for the two velocities after collision:

$$u_{sa} = \frac{(m_s u_{sb} - m_w u_{sb} + 2m_w u_{wb})}{(m_s + m_w)} \qquad \textit{eq. 25}$$

$$u_{wa} = \frac{(2m_s u_{sb} - m_s u_{wb} + m_w u_{wb})}{(m_s + m_w)} \qquad \textit{eq. 26}$$

The discrete "finite control volume" masses m, having lateral lengths dx and dy, are defined as follows:

$$m_s = \rho_s * dx * dy * H_s \qquad \textit{eq. 27}$$

$$m_w = \rho_w * dx * dy * H_w \qquad \textit{eq. 28}$$

Using this notation, the above expressions for velocity changes during collision can be rearranged in a form similar to the time- and space-discretized depth-averaged momentum equation:

$$\frac{\partial(\rho_s H_s u_s)}{\partial t} \approx \rho_s H_s (u_{sa} - u_{sb})/dt = \frac{2}{\left(\frac{1}{H_w \rho_w} + \frac{1}{H_s \rho_s}\right)} (u_{sb} - u_{wb})/dt \qquad \textit{eq. 29}$$

$$\frac{\partial(\rho_w H_w u_w)}{\partial t} \approx \rho_w H_w (u_{wa} - u_{wb})/dt = \frac{2}{\left(\frac{1}{H_w \rho_w} + \frac{1}{H_s \rho_s}\right)} (u_{sb} - u_{wb})/dt \qquad \textit{eq. 30}$$

where dt is the time discretization. Note that dx and dy are cancelled out. The right-hand sides of Eqs. (29) and (30) represent the momentum exchange source terms during collision.

The momentum transfer during the collision reference case was modified by a 'shape factor' S_F as a fitting parameter to reproduce the laboratory experiments from Miller et al. (2017), resulting in the following expressions:

$$M_{Ts} dt = S_F \frac{2}{\left(\frac{1}{H_w \rho_w} + \frac{1}{H_s \rho_s}\right)} (u_{wb} - u_{sb}) \qquad \textit{eq. 31}$$

$$M_{Tw} dt = -S_F \frac{2}{\left(\frac{1}{H_w \rho_w} + \frac{1}{H_s \rho_s}\right)} (u_{sb} - u_{wb}) \qquad \textit{eq. 32}$$

The shape factor S_F is defined from experiments to match the wave amplitude and the landslide deposit. This shape factor consists of a non-dimensional value that depends on the ratio between the maximum landslide thickness s_{max} at impact (recorded during the simulation by the numerical code) and the still water level h:

$$SF = 0.145(s_{max}/h)^{1.465} \qquad eq.\ 33$$

The choice of the values presented in Eq. (33) is a compromise to accurately fit the wave amplitude and the landslide deposit considering different still water levels. The deviation between the experiment and the numerical model using different value of FS (FS as in Eq. 33, FS + 50% and FS – 50%) are illustrated ~~Some values investigated in this process are presented~~ in Fig. 2.

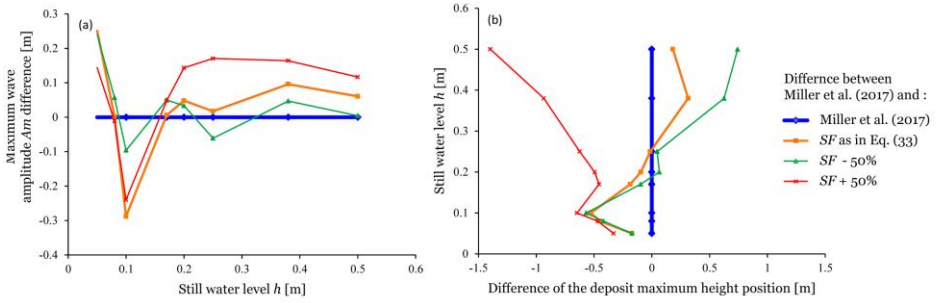

Figure 22: (a) Graph showing the difference between the A_m values from Miller et al. (2017) and Miller et al. (2017) (blue line) and the A_m values from the numerical simulation using different values in Eq. (33). Note that the value used in Eq. (33) (red line) is not the best fitting curve. (b) Graph showing the difference between the positions of the apex of the landslide deposits observed in Miller et al. (2017) and Miller et al. (2017) (blue line) and the positions obtained from the numerical simulations. ~~The best fitting values used in Eq. (33) are the values presented. The final choice of values is a compromise to accurately fit the wave amplitude and the landslide deposit.~~

~~**The set of equations presented in Mulligan and Take (2016) also describes the process of momentum transfer. However, the differences between their approach and our approach make comparisons difficult. On the one hand, our method is performed through time discretization, whereas the approach adopted by Mulligan and Take (2016) is performed in one "time step". Although this difference does not make the two approaches inherently incomparable, the equation proposed by Mulligan and Take (2016) defines the near-field maximum wave amplitude A_m as a function of the slide, the apparatus and the water body parameters (such as ρ_s, α, s, v_s, and h) whereas our equations define momentum transfer without change in height (Eqs. 25 & 26). In our code, the height change is obtained after, while solving the depth-averaged equations.**~~

4 Results

The landslide and the tsunami models are computed in 2D (x and y), whereas the results, such as the landslide thickness or the water elevation, ~~are~~ can be represented visually in the third dimension (z), or in other words, in 2.5D, as illustrated in Fig. 3.

Formatted: Font: Italic

Formatted: Font: Italic

Formatted: Caption

~~In this study, everything is computed as presented in Fig. 3, but the interpretations of the results are done through longitudinal cross-sections across the centre of the numerical flume (Fig. 4).~~

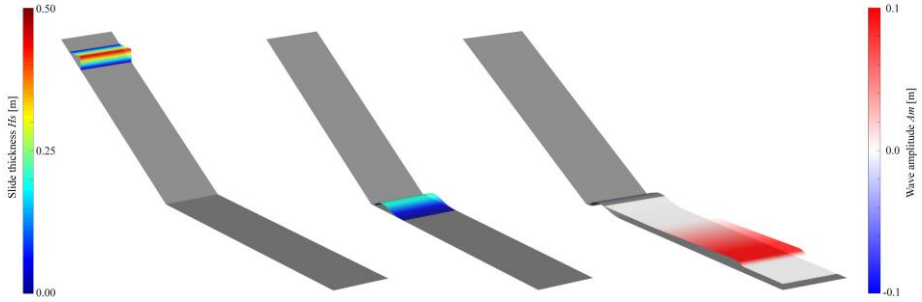

Figure 3: 2.5D numerical representation of the near-field section of the flume with water depth h = 0.2: (left) initial condition of the landslide (water level not displayed), (centre) landslide deposit (water level not displayed), and (right) landslide deposit (not coloured) with the generated wave.

Formatted: Font: Italic

Formatted: Normal

In this study, everything is computed in two-dimension, but the interpretations and the presentation of the results are done through longitudinal cross-sections across the centre of the numerical flume (Fig. 4). The Fig. 4 illustrate the generation of the wave: at 0 s, the landslide impacts the water; at 0.3 s, the landslide velocity is greater than the water velocity and the momentum is transferred; at 0.6 s, the front of the slide starts to stop while the back continues to transfer the momentum to the water; at 0.9, the momentum is nearly completed and the wave propagate along the flume.

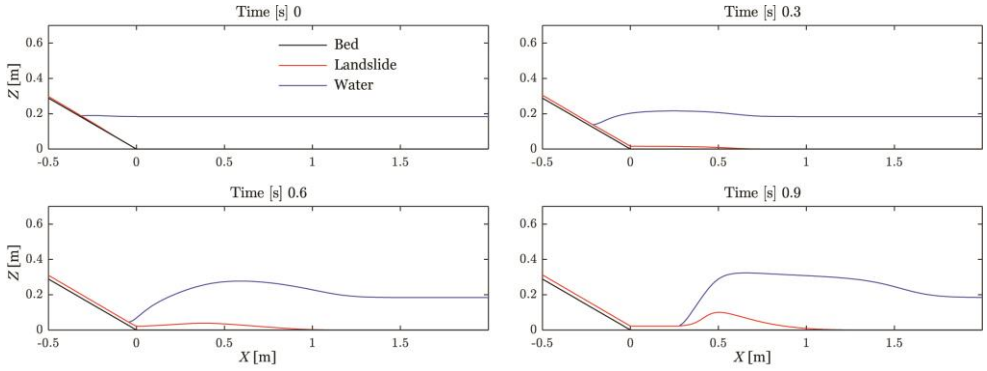

Figure 4: ~~Profile view~~Cross-section of the landslide and water surface during numerical simulation of the generation of the wave.

4.1 Landslide

This section presents the results concerning the granular landslide. Furthermore, this section discusses the behaviour of the landslide propagation using different rheological laws and the effect of the water depth on the landslide deposit.

4.1.1 Dry case

The dry case investigates the propagation of the granular material using various rheological laws. The rheological laws implemented herein are the Voellmy, Coulomb (flow with isotropic and anisotropic internal stresses) and Bingham rheological models. The velocities, the thicknesses and the deposit shapes obtained through the numerical simulation are compared to those data obtained from the physical experiment to identify and select the best solution.

Table 1: Rheological parameters used for the different rheological laws.

	Shear zone relative thickness [-]	Yield stress [Pa]	Dynamic viscosity [Pa·s]	Turbulence coefficient [m/s²]	Bed friction angle aluminium [°]	Bed friction angle concrete [°]	Int. friction angle [°]
	d_1	T_0	μ	ξ	Φ_{bed}	φ_{bed}	φ_{int}
Bingham	0.6	12	1.6	-	-	-	-
Voellmy	-	-	-	250	11	35	-
Coulomb (isotropic)	-	-	-	-	22	35	-
Coulomb (anisotropic)	-	-	-	-	22	35	33.7

The Bingham rheology is set by best fit with a shear zone relative thickness d_1 of 0.6, a yield stress T_0 of 12 Pa, and a dynamic viscosity μ of 1.6 Pa·s.

Concerning the Voellmy rheology, the determination of the turbulence coefficient ζ is performed by trial and error to obtain the best fit (back analysis). Thus, the turbulence coefficient ζ, as described in Hungr and Evans (1996) and in McDougall (2006), is set to 250 m/s^2. The bed friction angle φ_{bed} of 22°, given in Miller et al. (2017), was reduced to 11°. Indeed, the Voellmy rheology uses significantly lower values (Hungr and Evans, 1996). This study uses the same ratio (~0.5) between "classical" φ_{bed} and "Voellmy" φ_{bed} as the one presented in Hungr and Evans (1996) for cases with similar friction angles and turbulence coefficients ("Voellmy" φ_{bed} = 11°).

Regarding the two Coulomb models, we use the bed friction angle φ_{bed} of 22°, as measured in the physical experiment (Miller et al, 2017). In addition, the anisotropic Coulomb rheological model considers the internal friction angle φ_{int}, which is 33.7° (Miller et al, 2017).

In Miller et al. (2017), the velocity and the thickness of the landslide at impact are estimated through high-speed camera footage analysis with a still water depth h of 0.25 m. To measure the same variables of the simulated granular flow, the values are recorded using a corresponding window (Cam 1, Fig. 1).

Figure 5 shows the temporal evolution of the flow thickness and velocity captured at the numerical equivalent location of Cam 1 (Fig. 1). The numerical models do not fit the physical simulation very well. This poor fit can be explained by the

diffuse nature of a granular flow boundary that is not replicable by the shallow water assumption (continuum mechanics) and by the absence of expansion in the numerical moving mass. Nevertheless, the results from the numerical and physical models are ~~on the same order of magnitude,~~ close enough ~~which permits globally~~ to validat~~e~~ing globally the different numerical models ~~but does not allow~~without allowing their discrimination ~~between them~~.

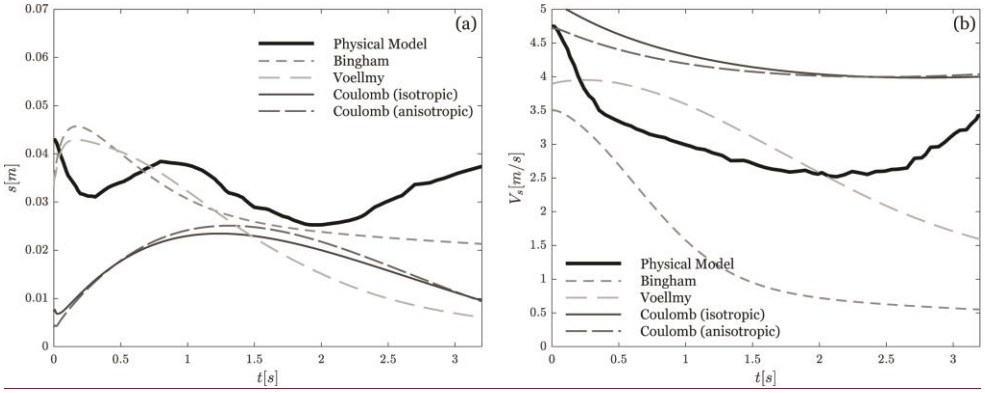

Figure 5: Landslide properties at impact (numerical equivalent location of Cam 1) with a still water depth h of 0.25 m. (a) Time series of slide thickness for different rheological laws (numerical model) compared with the mean thickness in the physical model. (b) Time series of depth-averaged slide velocity for different rheological laws (numerical model) v~~ersus~~ersus~~s.~~ the mean velocities in the physical model (modified from Miller et al., 2017).

Consequently, analysing the deposit (Fig. 6) is the way to identify ~~the~~ best fitting rheological model. The Bingham rheological model does not correctly reproduce the shape of a granular deposit. The Voellmy model performs better than the Bingham model in this respect, but in comparison with the two Coulomb frictional models, the Voellmy model is not satisfactory. Indeed, the two Coulomb rheological models (anisotropic and isotropic) fit the best with the observed deposit, which was expected because frictional rheological laws are typically developed to describe granular flows. The rear parts of the deposits are correctly located, whereas the fronts are slightly too distant. However, this imperfection is negligible and could be attributed to numerical diffusion. The deposit simulated with the isotropic Coulomb model is slightly closer to the real deposit than that simulated with the anisotropic model; this method has the advantage of being simple (only the bed friction angle φ_{bed} is implemented).

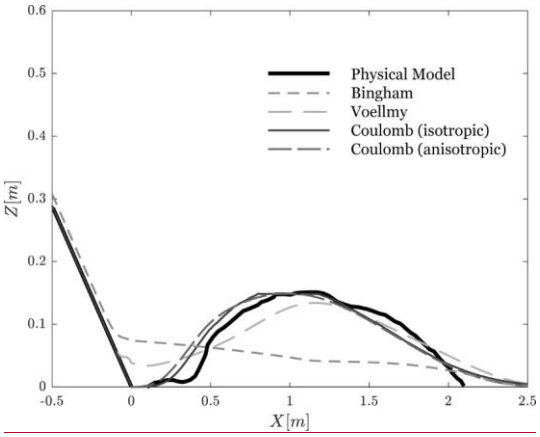

Figure 6: Cross-section of the landslide deposit using different rheological laws compared with the deposit in the physical experiment.

Since the velocities and the thickness are of a realistic magnitude, the deposit shapes of the two Coulomb models correctly reproduce the real case. Furthermore, due to the ease of implementation, the isotropic Coulomb model is the rheological model of choice. In ~~the~~ S~~s~~ect. 4.1.2, this model is used to study the wet cases.

4.1.2 Wet cases

This section investigates the interaction between the landslide and the water. More precisely, this section investigates the effect of the momentum transfer on the deposit shape for different water levels. Figure 7a shows the results for still water depths *h* of 0.05, 0.08, and 0.1 m. The deposits resulting from the numerical simulation (solid lines) are compared with the physical model observations (dashed lines), which shows a rather good similarity when focusing on the height of the piles. The numerical deposition shape for a still water depth of 0.05 m fits well the physical shape, also regarding the spread. Concerning still water depths *h* of 0.08 and the 0.1 m, the numerical granular flows stop further ~~more distantly~~ than the real flows.

At still water depths of 0.17, 0.2, and 0.25 m (Fig. 7b), the numerical and physical results are in good agreement; however, the "tails" and the apexes of the deposits are located slightly farther away in the numerical simulation.

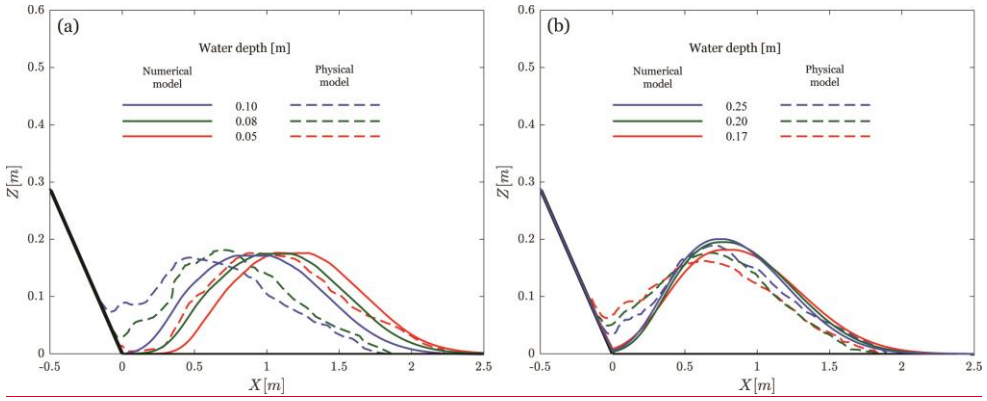

Figure 7: Cross-section of the granular flow deposit for different still water depths h (0.05 to 0.25 m)~~. The dashed lines represent the physical experiment observations~~ (modified from Miller et al., 2017~~), whereas the solid lines represent the results of the numerical model~~.

In contrast, for still water depths *h* of 0.38 and 0.5 m (Fig. 8), the deposit shapes obtained by the numerical simulations stop slightly ahead of the real deposits. Nevertheless, the deposits are of equivalent heights.

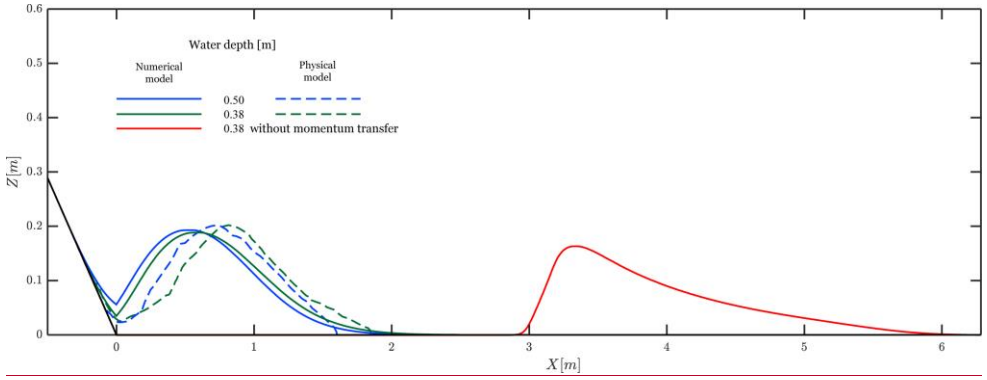

Figure 8: Cross-section of the granular flow deposit for two still water depths h (0.38 and 0.5 m). For comparison, the red line illustrates the landslide deposit for a still water depth h of 0.38 m without momentum transfer~~. The dashed lines represent the physical experiment observations, whereas the solid lines represent the results of the numerical model~~ (modified from Miller et al., 2017).

The momentum transfer acts correctly on the granular flow as the global correspondence between the numerical and physical deposition pattern is good. In fact, it is the combination of the momentum transfer (Eqs. 31 and~~&~~ 32) with the relative density ρ (Eqs. 7 ~~through~~ to 11) that performs well. This is highlighted by the simulated granular landslide without momentum transfer,

which travels excessively far (Figure 8~~Figure 8 8~~, red line). The travel distance in this case is even greater than that in the dry case (the result of the isotropic Coulomb model presented in Fig. 6) due to the effect of the relative density ρ. Indeed, the "drop in density" when the granular flow enters the water body reduces the total retarding stress T in particular (Eqs. 10 and~~&~~ 11; alongside P (Eq. 9) and GR (Eq. 8), which is negligible on flat surfaces). It is worth noting that without momentum transfer or relative density, the model would lead to the same deposit as the dry case.

4.2 Wave

This section investigates ~~the second aspect of~~ the momentum transfer between the slide and the ~~water~~generated wave~~: its effect on the generated wave.~~ This effect is analysed for different still water depths h (0.05, 0.1, 0.2, and 0.5 m) through probes located at different distances from the bottom of the slope (2.3, 15, and 23 m; Fig. 9). Concerning the case with the smallest still water depth (h = 0.05 m), the numerical simulation reproduces the wave observed in the physical experiment very well in terms of amplitude and timing at each probe. Note that the simulated wave is taller than the real wave in the very near field (2.3 m gauge). For a still water depth h of 0.1 m, the timing is good at the 2.3 m gauge, but, as previously described, the numerical wave is taller. Concerning the gauges at 15 and 23 m, the wave celerity is faster and its amplitude is smaller in the numerical simulation than in the physical experiment. Moreover, the wave train observed in the physical model is non-existent in the numerical model. Except for the equivalence in amplitude in the near field, the same observations apply for a still water depth h of 0.2 m. For a still water depth of 0.2 m, a reflected wave is present at the 23 m gauge after approximately 23 s. The numerically simulated wave arrives slightly earlier than the observed wave. Concerning the case of a still water depth h of 0.5 m, the simulated wave is slightly smaller than the real wave, and the reflected wave (at 28, 23, and 18 s) is visible at the 3 gauge locations with a good correspondence in terms of time.

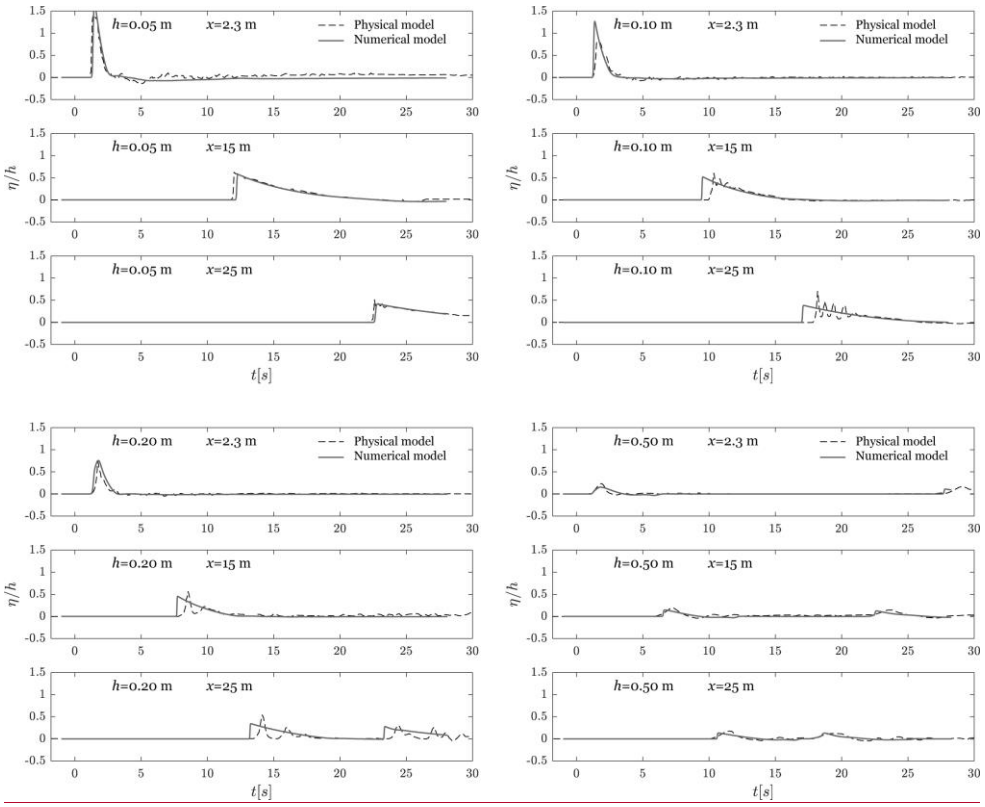

Figure 9: Time series of the relative water surface elevation η/h for different still water depths *h* (.0.05, 0.10, 0.20 and 0.50 m) observed at different wave probes/gauges (2.3, 15, and 25 m)~~). The dashed lines represent the physical experiment observations, whereas the solid lines represent the results of the numerical model~~ (modified from Miller et al., 2017).

~~4.2.1 Runup~~

~~Figure 10 presents the comparison of the runup height *R* as a function of the maximum amplitude A_m at the 25 m gauge between the physical experiments and the numerical simulation. Even if the wave is breaking with water depths of 0.38 and 0.5 m in the physical experiment, the match is adequate between the physical experiment and the simulation. Moreover, the underestimation of A_m for the 0.1–0.25 m water level can be explained by the wave train that occurs in the flume but not in the numerical simulation. We can underline that there is a better match with the runup height than with the wave amplitude. This~~

~~phenomenon can be explained by the fact that when a wave train is present, it produces a higher frontal wave but that the volume of displaced water is similar (trough and crest compensate) and hence a similar runup height.~~

~~**Figure 10: Runup on a smooth impermeable slope of 27°. Runup height as a function of the incident wave maximum amplitude A_m at the 25 m gauges. The coloured hollow shapes represent the results of the numerical model, whereas the solid greyscale shapes are the observed values from the physical model (modified from Miller et al., 2017).**~~

4.2.1 Impulse product parameter

Heller and Hager (2010) proposed a relationship between the landslide characteristics and the near-field maximum amplitude of the generated wave through the concept of the impulse product parameter *P*. The impulse produce parameter includes the governing parameters related to the landslide and the still water depth. The maximum wave amplitude can be predicted as a function of *P* through Eq. (37). This approach is relevant to our study because it inherently considers the momentum transfer occurring during wave generation. The following values are captured at the impact zone (Cam 1, Fig. 1) for the sliding mass and in the near-field area for the wave. The relative maximum near-field wave amplitude A_m is defined by the following expression:

$$A_m = 0.25\, Fr^{1.4}\, S^{0.8} \qquad \textit{eq. 34}$$

where *S* is the relative landslide thickness and *Fr* is the Froude number, which are defined as follows:

$$S = s_{max}/h \qquad \textit{eq. 35}$$

$$Fr = u_s/\sqrt{(gh)} \qquad \textit{eq. 36}$$

The relationships between the impulse product parameter and the Froude number and the relative landslide thickness were found empirically through a large set of tests based on different ~~reservoir and~~ landslide setups (Fritz et al., 2004). The impulse product parameter *P* defined by Heller and Hager (2010) is expressed as follows:

$$P = Fr\, S^{1/2}\, M^{1/4} \left\{cos\left[\left(6/7\right)\alpha\right]\right\}^{1/2} \qquad \textit{eq. 37}$$

where *M* is the relative landslide mass, which is defined by the following expression:

$$M = m_s/(\rho_w b h^2) \qquad \textit{eq. 38}$$

where m_s is the landslide mass and *b* is the flume width. The near-field relationship between the *P* and A_m is defined as follows (Heller and Hager, 2010):

$$A_M = \frac{4}{9}P^{4/5} \qquad eq.\ 39$$

Figure 1~~1~~0 shows this relationship with the results of Miller et al. (2017) alongside the results of the present study. The two dashed lines represent the same relationship ± 30%. A large set of data collected in flume experiments (Fritz et al., 2004; Heller and Hager, 2010) falls between those limits for P<9.

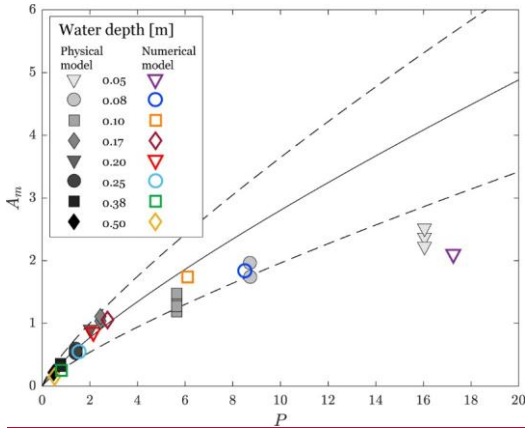

Figure 1~~0~~1: Maximum relative wave amplitude A_m as a function of the impulse product parameter P. (solid line) A_M from Eq. (39), (dashed lines) A_M from Eq. (39) ± 30%, (solid shapes) data from the physical model (Miller et al. 2017), and (hollow shapes) data from the numerical simulation (this study).

The near-field relationships between P and A_m obtained in the present study correspond very well with those obtained by Miller et al. (2017) (Fig. 1~~0~~1). On the other hand, for P<9 (as originally presented in Heller and Hager, 2010), the results of this study are located within a range of ±30%.

4.3 Computation time

Formatted: Heading 2

All the simulations are performed on a conventional computer. It is an Acer Aspire V17 Nitro. The computations are performed on an Intel® Core ™ i7-7700HQ CPU @ 2.80GHz with 16 Go of RAM. For a complete simulation, i.e. simulation that include landslide and wave propagation, for a duration of 30 s (as presented in Fig. 9), the computation time is of 16'650 s. The cell size is 0.01 x 0.01 m and the grid size is 45.2 m x 2.1 m (949'000 cells).

4.~~3~~3 Discussion

The numerical model displays a taller wave in the near field, which can be explained by the fact that the model does not reproduce the breaking of the wave. This lack also implies that the model cannot consider the impact crater as long as the

steepness of the water surface is not steeper than sub-vertical. This discrepancy is inherent to the shallow water model and its two-dimensional nature. ~~This finding is supported by the fact that this phenomenon is observed for still water depths *h* of 0.05-0.17 m, which are depths prone to wave breaking in the Miller et al. (2017) experiments.~~

The physical experiments produce wave trains for water levels of 0.1 and 0.2 m. This phenomenon is not reproduced by the numerical model because of~~; this finding could be explained by~~ the absence of breaking in the unstable numerical waves, ~~which is the cause of the aforementioned train~~ (Miller et al. 2017; Ruffini et al. 2019) along with the lack of frequency dispersion (Ruffini et al. 2019)~~. It is clear that the complex interaction between the landslide and the presence of possible small-scale backwash during generation is not the cause. Indeed, the "unique" wave at the 2.3 m probe, which is farther than the slide deposit, verifies that the apparition of the train occurs after the wave generation (Miller et al. 2017).~~ These mismatches are due to the incomplete physics inherent to shallow water equations approximations.

On the other hand, the fronts of the waves ~~is~~ are very different. The "excess" volume of water at the front of the numerical wave is also partially explained by the lack of energy dissipation that would occur during breaking. On average, the simulated water level located at the wave train "match" the trough and the crests. For those cases, the imperfect reproductions are, however, sufficiently close in terms of celerity and volume to be considered relevant. This consideration was ~~further~~ in addition confirmed by the good match of the reflected wave (e.g. Fig. 9, h=0.2, x=25, 23 s)~~. and the measured runup (Fig. 10).~~

The general observation of the evolution of the wave (Fig. 9) shows that the decay occurring in the physical experiment is present in the numerical simulation. This fact also strengthens the general validity of the whole numerical model.

Inherently, as the impulse product parameter values obtained through a wide set of experiments (Heller and Hager, 2010; Miller et al., 2017) fall into an envelope of ±30%, our near-field results, which also fall into these limits, strongly confirm the validity of our model and our momentum transfer approach.

Formatted: Font: Italic

Formatted: Font: Italic

5 Conclusions

This study aimed to validate our two-layer landslide-generated tsunami numerical model, based on the shallow water equations, particularly concerning the momentum transfer between the landslide and the water. This is performed through the reproduction of the physical experiments conducted by Miller et al. (2017). A dry case is simulated to document the behaviour of the landslide propagation model using different rheological laws. In addition, a wet case is reproduced to investigate the influence of different still water levels on both the landslide deposit and the generated waves.

The dry case shows that the two Coulomb rheological models (flow with isotropic or anisotropic internal stresses) correctly reproduce the deposit observed in the physical model studied by Miller et al. (2017). The isotropic Coulomb model is the simplest and easiest to implement and is chosen to study the wet case.

The numerical simulation of the wet case investigates the abilities of the model to correctly handle momentum transfer. This case focuses on both the effect of the water on the landslide deposit and the effect of the landslide on the resulting wave. These effects are investigated through different water levels, and it appears that the landslide deposit obtained by the numerical

simulations fits well with the physical model observations. On the other hand, the numerical waves behave similarly to the waves in the physical model. Despite imperfections, the combined results from investigating these two effects permits us to consider that, overall, the model effectively handles the complex phenomenon occurring during the interaction between the landslide and the water. In addition, the choice to transfer the momentum through the simple ~~perfectly elastic~~ "perfect" collision principle is verified to be relevant.

A comparison involving the impulse product parameter~~s~~ particularly highlights that our model satisfactorily reproduces the physical experiment of Miller et al. (2017). The values of A_m versus P presented in Heller and Hager (2010) are based on their 211 experiments in addition with ~~223~~ 137 ~~sets of flume~~ experiments performed by Fritz et al. (2002) and 86 by Zweifel (2004). Hence, the validity of our model is further strengthened by the fact that the results of our model also fit well with those experiments.

Finally, our model is validated by a benchmark test performed herein, as this approach is very simple to implement and is very efficient in terms of computational resources. Therefore, we consider our model as a tool of choice for the assessment of landslide-generated tsunami hazards.

Author contributions. MF and MJ conceived the project. MF MJ RM and AT designed the benchmark tests. MF and YP developed the model code, RM ant AT provided the data and MF carried out the simulations. MF prepared the manuscript with review and editing from ~~the~~ all co-authors.

Competing interests. The authors declare that they have no conflict of interest.

Acknowledgements. The authors are thankful to Dr. Shiva P. Pudasaini for sharing his valuable insights about landslides impacting water bodies, particularly on the associated complexity of momentum transfer. We acknowledge two anonymous reviewers for their constructive comments.

Notation

The following symbols are used in this paper:

A_m	=	maximum measured wave amplitude ~~of measured wave~~ [m]
A_M	=	theoretical maximum wave amplitude ~~of~~ in the near-field ~~wave~~ [m]
B	=	bed elevation [m]
b	=	flume width [m]
C	=	Chézy coefficient [-]
d_1	=	shear layer relative thickness [-]
F	=	flux vector in x direction [-]

Fr	=	Froude number [-]
G	=	flux vector in y direction [-]
g	=	gravitational acceleration [m/s^2]
GR	=	driving component of gravity [Pa]
H	=	layer depth [m]
h	=	still water level [m]
h_{min}	=	minimum water thickness (ultrathin layer) [m]
H_s	=	landslide thickness [m]
H_{sa}	=	landslide thickness after collision [m]
H_{sb}	=	landslide thickness before collision [m]
H_w	=	depth of the water [m]
H_{wa}	=	depth of the water after collision [m]
H_{wb}	=	depth of the water before collision [m]
K	=	earth pressure coefficient [-]
LF	=	Lax-Friedrichs scheme
M	=	relative landslide mass [-]
m_s	=	landslide mass [kg]
MT_s	=	momentum transfer (water to ~~->~~slide) [Pa]
MT_w	=	momentum transfer (slide to ~~->~~water) [Pa]
n	=	Manning roughness coefficient [-]
P	=	pressure term [Pa]
P	=	impulse product parameter [-]
~~R~~	~~=~~	~~runup height [m]~~
Re	=	Reynolds number [-]
Re_{tr}	=	Re threshold [-]
S	=	source term [-]
S	=	relative landslide thickness [-]
SF	=	shape factor for momentum transfer [-]
s_{max}	=	maximum landslide thickness [m]
T	=	total retarding stress [Pa]
T_0	=	yield stress [Pa]
U	=	s~~S~~olution vector [-]
u	=	velocity vector component in x direction [m/s]
u_s	=	landslide velocity in x direction [m/s]
u_{sa}	=	landslide velocity in x direction after collision [m/s]
u_{sb}	=	landslide velocity in x direction before collision [m/s]

u_w	=	water velocity in x direction [m/s]
u_{wa}	=	water velocity in x direction after collision [m/s]
u_{wb}	=	water velocity in x direction before collision [m/s]
v	=	velocity vector component in y direction [m/s]
V	=	full velocity vector [m/s]
v_s	=	landslide velocity in y direction [m/s]
v_w	=	water velocity in y direction [m/s]
x	=	longitudinal coordinate [m]
y	=	transverse coordinate [m]
z	=	vertical coordinate [m]
α	=	bed slope angle [°]
Δt	=	time step [s]
η	=	wave amplitude [m]
μ_s	=	landslide dynamic viscosity [Pa s]
μ_w	=	water dynamic viscosity [Pa s]
ξ	=	turbulence coefficient [m/s^2]
ρ	=	~~relative~~ apparent density [-]
ρ_s	=	landslide bulk density [kg/m^3]
ρ_{sa}	=	landslide bulk density after collision [kg/m^3]
ρ_{sb}	=	landslide bulk density before collision [kg/m^3]
ρ_w	=	water density [kg/m^3]
ρ_{wa}	=	water density after collision [kg/m^3]
ρ_{wb}	=	water density before collision [kg/m^3]
φ_{bed}	=	bed friction angle [°]
φ_{int}	=	internal friction angle [°]

References

Abadie, S., Morichon, D., Grilli, S., and Glockner, S.: Numerical simulation of waves generated by landslides using a multiple-fluid Navier-Stokes model. Coastal Engineering, 57 (9), 779–794, 2010.

Bosa, S. and Petti, M.: Shallow water numerical model of the wave generated by the Vajont landslide. Environ. Modell. Softw., 26(4), 406-418, https://doi.org/10.1016/j.envsoft.2010.10.001, 2011.

Clous, L. and Abadie, S.: Simulation of energy transfers 935 in waves generated by granular slides. Landslides, 1–17, 2019.

Crosta, G. B., Imposimato, S., and Roddeman, D.: Monitoring and modelling of rock slides and rock avalanches, in: International Conference Vajont 1963-2013. Thoughts and analyses after 50 years since the catastrophic landslide, edited by: Genevois, R. and Prestininzi, A., Italian Journal of Engineering Geology and Environment – Book Series (6), Sapienza Università Editrice, Rome, Italy, 3-14, 2013.

Enet, F. and Grilli, S. T.: Experimental ~~S~~study of tsunami ~~s~~Generation by ~~t~~Three-~~d~~Dimensional ~~r~~Rigid ~~u~~Undewater ~~l~~Landslide, J. Waterw. Port Coast., 133(6), 442-454, https://doi.org/10.1061/(ASCE)0733-950X(2007)133:6(442), 2007.

Fischer, J. T., Kowalski, J., and Pudasaini, S. P.: Topographic curvature effects in applied avalanche modeling. Cold Reg. Sci. Technol., 74, 21-30, https://doi.org/10.1016/j.coldregions.2012.01.005, 2012.

Franz, M., Podladchikov, Y., Jaboyedoff, M., and Derron, M.-H.: Landslide-Triggered Tsunami Modelling in Alpine Lakes, in: International Conference Vajont 1963-2013. Thoughts and analyses after 50 years since the catastrophic landslide, edited by: Genevois, R. and Prestininzi, A., Italian Journal of Engineering Geology and Environment – Book Series (6), Sapienza Università Editrice, Rome, Italy, 409-416, https://doi.org/10.4408/IJEGE.2013-06.B-39, 2013.

Franz, M., Jaboyedoff, J., Podladchikov, Y., and Locat, J.: Testing a landslide-genrated tsunami model. The case of the Nicolet Landslide (Québec, Canada), in: Proceeding of the 68th Canadian Geotechnical Conf., GEOQuébec 2015, Québec City, Canada, 2015.

Franz, M., Carrea, D., Abellán., A., Derron, M.-H., and Jaboyedoff, M.: Use of targets to track 3D displacements in highly vegetated areas affected by landslide, Landslides, 13, 821-831, https://doi.org/10.1007/s10346-016-0685-7, 2016.

Franz, M., Rudaz, B., Jaboyedoff, M., and Podladchikov, Y.: Fast assessment of landslide-generated tsunami and associated risks by coupling SLBL with shallow water model, in: Proceeding of the 69th Canadian Geotechnical Conf., GEOVancouver 2016, Vancouver, Canada, 2016.

Fritz, H. M., Hager, W. H., and Minor, H.-E.: Near field characteristics of landslide generated impulse waves, J. Waterw. Port Coast., 130(6), 287–302, 2004.

Fritz, H. M., Mohammed, F., and Yoo, J.: Lituya Bay Landslide Impact Generated Mega-Tsunami 50(th) Anniversary, Pure Appl. Geophys., 166(1-2), 153-175, https://doi.org/10.1007/s00024-008-0435-4, 2009.

Ganerød, G. V., Grøneng, G., Rønning, J. S., Dalsegg, E., Elvebakk, H., Tønnesen, J. F., Kveldsvik, V., Eiken, T., Blikra, L. H., and Braathen, A.: Geological model of the Åknes rockslide, western Norway, Eng. Geol., 102(1–2), 1-18, 2008.

Ghetti, A.: Esame sul modello degli effetti di un'eventuale frana nel lago-serbatoio del Vajont. Istituto di Idraulica e Costruzioni Idrauliche dell'Università di Padova. Centro modelli idraulici « E. Scimemi ». S.A.D.E. Rapporto interno inedito, 12pp, 14 fotographie, 2 tabelle, 8 tavole, Venezia, 1962.

Ghirotti, M., Masetti, D., Massironi, M., Oddone, E., Sapigni, M., Zampieri, D., and Wolter, A.: The 1963 Vajont Landslide (Northeast Alps, Italy) - Post-Conference Field trip (october 10th, 2013), in: International Conference Vajont 1963-2013. Thoughts and analyses after 50 years since the catastrophic landslide, edited by: Genevois, R. and Prestininzi, A., Italian Journal of Engineering Geology and Environment – Book Series (6), Sapienza Università Editrice, Rome, Italy, 2013.

Harbitz, C. B., Glimsdal, S., Løvholt, F., Kveldsvik, V., Pedersen, G. K., and Jensen, A.: Rockslide tsunamis in complex fjords: From an unstable rock slope at Åkerneset to tsunami risk in western Norway, Coast. Eng., 88(0), 101-122, https://doi.org/10.1016/j.coastaleng.2014.02.003, 2014.

Heller, V. and Hager, W. H.: Impulse product parameter in landslide generated impulse waves, J. Waterw. Port Coast., 136(3), 145–155, 2010.

Heller, V., Hager, W. H., and Minor, H.-E.: Landslide generated impulse waves in reservoirs: Basics and computation, VAW Manual 4257, Laboratory of Hydraulics, Hydrology and glaciology, ETHZ, Zürich, Switzerland, 172 pp., 2009.

Heller, V., Bruggemann, M., Spinneken, J., and Rogers, B. D.: Composite modelling of subaerial landslide–tsunamis in different water body geometries and novel insight into slide and wave kinematics, Coast. Eng., 109, 20-41, https://doi.org/10.1016/j.coastaleng.2015.12.004, 2016.

Hungr, O. and Evans, S. G.: Rock avalanche runout prediction using dynamic model, in: Proceedings of the 7th International Symposium on Landslides, Trondheim, Norway, 233-238, 1996.

Hungr, O. and McDougall, S.: Two numerical models for landslide dynamic analysis, Comput. Geosci., 35(5), 978-992, https://doi.org/10.1016/j.cageo.2007.12.003, 2009.

Iverson R. M.: The Physics of debris flows, Rev. Geophys., 35(3), 245-296, https://doi.org/10.1029/97RG00426, 1997.

Jaboyedoff, M., Demers, D., Locat, J., Locat, A., Locat, P., Oppikoffer, T., Robitaille, D., and Turmel, D.: Use of terrestrial laser scanning for the characterization of retrogressive landslide in sensitive clay and rotational landslides in river banks, Can. Geotech. J., 46(12), 1379-1390, https://doi.org/10.1139/T09-073, 2009.

Kafle, J., Kattel, P., Mergili, M., Fischer, J. T., and Pudasaini, S. P.: Dynamic response of submarine obstacles to two-phase landslide and tsunami impact on reservoirs, Acta Mech., 230(9), 3143-3169, 2019.

Kamphuis, J. W. and Bowering, R. J.: Impulse waves generated by landslides, in: Proceedings of the 11th Coastal Engineering Conference, 575-588, 1970.

Kelfoun, K.: Suitability of simple rhological laws for the numerical simulation of dense pyroclastic flows and long-runout volcanic avalanches, J. Geophys. Res., 116, https://doi.org/10.1029/2010JB007622, 2011.

Kelfoun, K., Giachetti, T., and Lazabazuy, P.: Landslide-generated tsunami at Réunion Island, J. Geophys. Res., 115, https://doi.org/10.1029/2009JF001381, 2010.

Kremer, K., Simpson, G., and Girardclos, S.: Giant Lake Geneva tsunami in AD 563, Nat. Geosci., 5(11), 756-757, https://doi.org/10.1038/ngeo1618, 2012.

Kremer, K., Marillier, F., Hilbe, M., Simpson, G., Dupuy, D., Yrro, B. J., Rachoud-Schneider, A.-M., Corboud, P., Bellwald, B., and Wildi, W.: Lake dwellers occupation gap in Lake Geneva (France–Switzerland) possibly explained by an earthquake–mass movement–tsunami event during Early Bronze Age. Earth. Planet. Sc. Lett., 385, 28-39, https://doi.org/10.1016/j.epsl.2013.09.017, 2014.

L'Heureux, J.-S., Eilertsen, R. S., Glimsdal, S., Issler, D., Solberg, I.-L., and Harbitz, C. B.: The 1978 quick clay landslide at Rissa, mid Norway: subaqueous morphology and tsunami simulations, in: Submarine Mass Movements and Their Consequences, edited by: Yamada, Y., Kawamura, K., Ikehara, K., Ogawa, Y., Urgeles, R., Mosher, D., Chaytor, J., and Strasser, M., Springer, 507-516, 2012.

Lacasse, S., Eidsvig, U., Nadim, F., Høeg, K., and Blikra, L. H.: Event tree analysis of Åknes rock slide hazard, in: Proceedings of the 4th Canadian Conference on Geohazards, Université Laval, Québec City, Canada, 20-24, 2008.

Longchamp, C., Caspar, O., Jaboyedoff, M., and Podlachikov, Y.: Saint-Venant Equations and Friction Law for Modelling Self-Channeling Granular Flows: From Analogue to Numerical Simulation, Applied Mathematics, 6(07), 1161-1173, http://dx.doi.org/10.4236/am.2015.67106, 2015.

Løvholt, F., Lynett, P., and Pedersen, G. K.: Simulating run-up on steep slopes with operational Boussinesq models; capabilities, spurious effects and instabilities, Nonlin. Processes Geophys., 20, 379–395, https://doi.org/10.5194/npg-20-379-2013, 2013.

Løvholt, F., Glimsdal, S., Lynett, P., and Pedersen, G.: Simulating tsunami propagation in fjords with long-wave models. Natural Hazards & Earth System Sciences, 15(3), 2015.

Ma, G., Kirby, J. T., Hsu, T.-J., and Shi, F.: A two-layer granular landslide model for tsunami wave generation: Theory and computation. Ocean Modelling 93:40-55, 2015.

Mandli, K. T.: A Numerical Method for the Two Layer Shallow Water Equations with Dry States, Ocean Model., 72, 80–91. 2013.

McDougall, S.: A New Continuum Dynamic Model for the Analysis of Extremely Rapid Landslide Motion across Complex 3D Terrain, Ph.D. thesis, University of British Columbia, Vancouver, Canada, 2006.

Miller, G. S., Take, W. A., Mulligan, R. P., and McDougall, S.: Tsunami generated by long and thin granular landslides in a large flume, J. Geophys. Res.-Oceans, 122, 653-668, https://doi.org/10.1002/2016JC012177, 2017.

Mulligan, R. P. and Take, W. A.: On the transfer of momentum from a granular landslide to a water wave, Coast. Eng., 125, 16-22, https://doi.org/10.1016/j.coastaleng.2017.04.001, 2016.

Mulligan, R. P., Take, W. A., and Miller, G. S.: Propagation and runup of tsunami generated by gravitationally accelerated granular landslides, in: Proceeding of the 6th International Conference on the Application of Physical Modelling in Coastal and Port Engineering and Science (Coastlab16), International Association for Hydro-Environment Engineering and Research (IAHR), Ottawa, Canada, 10-13 May 2016, 6 pp., 2016.

Pudasaini, S. P.: A general two-phase debris flow model, J. Geophys. Res.-Earth, 117(F03010), https://doi.org/10.1029/2011JF002186, 2012.

Pudasaini, S. P. and Hutter, K. (Eds.): Avalanche Dynamics: Dynamics of rapid flows of dense granular avalanches, Springer Science & Business Media, Berlin, Heidelberg, Germany, 2007.

Pudasaini, S. P. and Krautblatter, M.: A two-phase mechanical model for rock-ice avalanches, J. Geophys. Res.-Earth, 119(10), 2272-2290, https://doi.org/10.1002/2014JF003183, 2014.

Pouliquen, O. and Forterre, Y.: Friction law for dense granular flows: application to the motion of a mass down a rough inclined plane, J. Fluid Mech., 453, 133-151, 2001.

Roberts, N. J., McKillop, R. J., Lawrence, M. S., Psutka J. F., Clague, J. J., Brideau, M.-A., and Ward, B. C.: Impact of the 2007 Landslide-Generated Tsunami in Chehalis Lake, Canada, in : Landslide Science and Practice, edited by: Margottini, C., Canuti, P., and Sassa, K., Springer, Berlin, Heidelberg, Germany, 133-140, https://doi.org/10.1007/978-3-642-31319-6_19, 2013.

Ruffini, G., Heller, V., and Briganti, R.: Numerical modelling of landslide-tsunami propagation in a wide range of idealised water body geometries. Coastal Engineering 153:103518, 2019.

Schnellmann, M., Anselmetti, F. S., Giardini, D., and McKenzie, J. A.: 15,000 Years of mass-movement history in Lake Lucerne: Implications for seismic and tsunami hazards, Eclogae Geol. Helv., 99(3), 409-428, 2006.

Simpson, G. and Castelltort, S.: Coupled model of surface water flow, sediment transport and morphological evolution, Computer & Geoscience, 32, 1600-1614, 2006.

Skvortsov, A.: Numerical Simulation of Landslide-Generated Tsunamis with Application to the 1975 Failure in Kitimat Arm, British Columbia, Canada, MSc. thesis, University of Victoria, Victoria, Canada, 2005.

Slingerland, R. L. and Voight, B.: Occurrences, Properties, and Predictive Models of Landslide-Generated Water Waves, in: Rockslides and Avalanches, 2: Engineering Sites, Developments in Geotechnical Engineering vol. 14B, edited by: Voight, B., Elsevier, Amsetrdan, The Netherlands, 317-394, 1979.

Tappin, D. R., Watts, P., and Grilli, S. T.: The Papua New Guinea tsunami of 17 July 1998: anatomy of a catastrophic event, Nat. Hazard Earth Sys., 8(2), 243-266, https://doi.org/10.5194/nhess-8-243-2008, 2008.

Tan, H., Ruffini, G., Heller, V., and Chen, S.: A numerical landslide-tsunami hazard assessment technique applied on hypothetical scenarios at Es Vedrà, offshore Ibiza. Journal of Marine Science and Engineering 6(4):1-22, 2018.

Tinti, S. and Tonini, R.: The UBO-TSUFD tsunami inundation model: validation and application to a tsunami case study focused on the city of Catania, Italy, Nat. Hazard Earth Sys., 13(7), 1795–1816, https://doi.org/10.5194/nhess-13-1795-2013, 2013.

Tinti, S., Pagnoni, G., and Zaniboni, F.: The landslides and tsunamis of the 30th of December 2002 in Stromboli analysed through numerical simulations, B. Volcanol., 68, 462–479, 2006.

Tinti, S., Zaniboni, F., Pagnoni, G., and Manucci, A.: Stromboli Island (Italy): Scenarios of Tsunami Generated by Submarine Landslide, Pure Appl. Geophys., 165(11-12), 2143-2167, https://doi.org/10.1007/s00024-008-0420-y 2008.

Toro, E. F.: Shock-Capturing Methods for Free-Surface Shallow Flows, Wiley, New York, 2001.

Turcotte, D. L. and Schubert, G. (Eds.): Geodynamics: 2nd Edition, Cambridge University Press, 472pp., 2002.

Voellmy, A.: Uber die Zerstörungskraft von Lawinen, Schweizerische Bauzeitung, 73, 212-285, 1955.

Ward, S. N.: Landslide tsunami, J. Geophys. Res.-Earth, 106(6), 11201– 11215, https://doi.org/10.1029/2000JB900450, 2001.

Ward, S. N. and Day, S.: The 1963 Landslide and Flood at Vaiont Reservoir Italy. A tsunami ball simulation, Ital. J. Geosci., 130(1), 16-26, https://doi.org/10.3301/IJG.2010.21, 2011.

Wei, Z., Dalrymple, R. A., Hérault, A., Bilotta, G., Rustico, E., and Yeh, H.: SPH modeling of dynamic impact of tsunami bore on bridge piers, Coast. Eng., 104, 26-42, 2015.

Weiss, R., Fritz, H. M., and Wünnemann, K.: Hybrid modeling of the mega-tsunami runup in Lituya Bay after half a century, Geophys. Res. Lett., 36(9), https://doi.org/10.1029/2009GL037814, 2009.

Xiao, L., Ward, S., and Wang, J.: Tsunami Squares Approach to Landslide-Generated Waves: Application to Gongjiafang Landslide, Three Gorges Reservoir, China, Pure Appl. Geophys., 172, 3639-3654, 2015.

Formatted: English (United Kingdom)